Accepted article: Cleverly J, Eamus D, Restrepo Coupe N, Chen C, Maes W, Li L, Faux R, Santini NS, Rumman R, Yu Q, Huete A. 2016. Soil moisture controls on phenology and productivity in a semi-arid critical zone. *Science of the Total Environment*. DOI: 10.1016/j.scittotenv.2016.05.142.

http://www.sciencedirect.com/science/article/pii/S0048969716310725

Soil moisture controls on phenology and productivity in a semi-arid critical zone

Special issue: *Landscape evolution and intensification in Australia: The Living Critical Zone perspective*

James Cleverly[1,2], Derek Eamus[1,2], Natalia Restrepo Coupe[1,3], Chao Chen[4], Wouter Maes[1,3], Longhui Li[1], Ralph Faux[1], Nadia S Santini[1], Rizwana Rumman[1], Qiang Yu[1], Alfredo Huete[1,3]

[1]{School of Life Sciences, University of Technology Sydney, PO Box 123, Broadway, NSW, 2007, Australia}

[2]{Australian SuperSite Network, University of Technology Sydney}

[3]{Plant Functional Biology and Climate Change Cluster, University of Technology Sydney}

[4]{CSIRO Agriculture Flagship, PMB 5, PO Wembley, WA, 6913, Australia}

Correspondence to: J. Cleverly (james.cleverly@uts.edu.au)

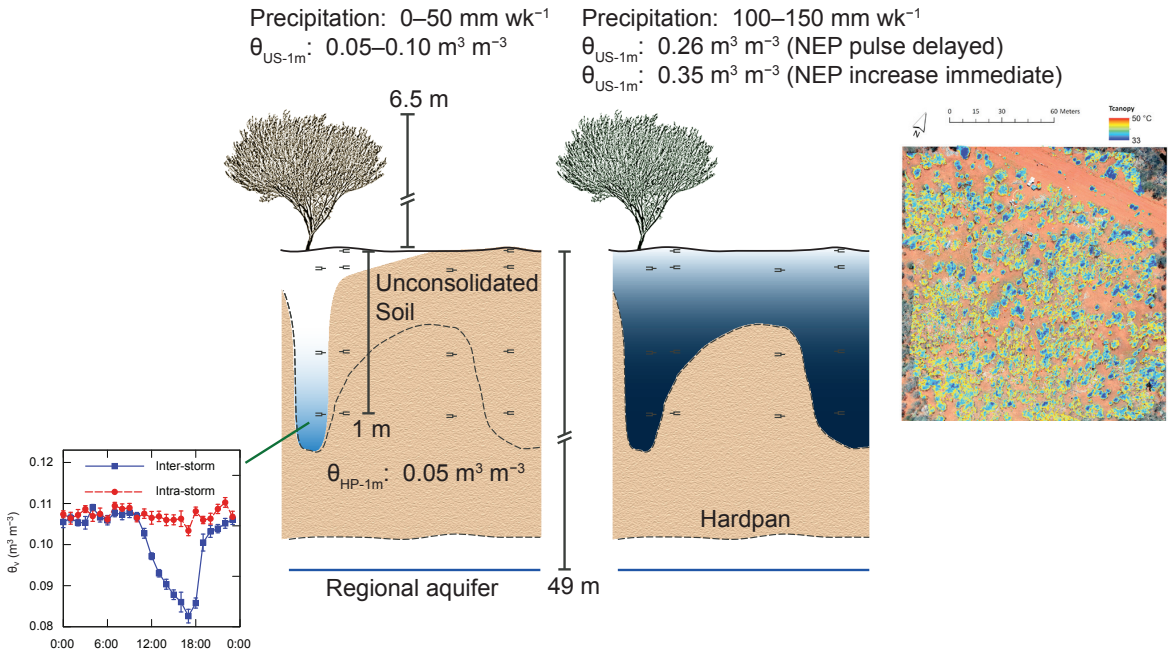

Abstract

The Earth's Critical Zone, where physical, chemical and biological systems interact, extends from the top of the canopy to the underlying bedrock. In this study, we investigated soil moisture controls on phenology and productivity of an *Acacia* woodland in semi-arid central Australia. Situated on an extensive sand plain with negligible runoff and drainage, the carry-over of soil moisture content (θ) in the rhizosphere enabled the delay of phenology and productivity across seasons, until conditions were favourable for transpiration of that water to prevent overheating in the canopy. Storage of soil moisture near the surface (in the top few metres) was promoted by a siliceous hardpan. Pulsed recharge of θ above the hardpan was rapid and depended upon precipitation amount: 150 mm storm^{-1} resulted in saturation of θ above the hardpan (i.e., formation of a temporary, discontinuous perched aquifer above the hardpan in unconsolidated soil) and immediate carbon uptake by the vegetation. During dry and inter-storm periods, we inferred the presence of hydraulic lift from soil storage above the hardpan to the surface due to (i) regular daily drawdown of θ in the reservoir that accumulates above the hardpan in the absence of drainage and evapotranspiration; (ii) the dimorphic root distribution wherein most roots were found in dry soil near the surface, but with significant root just above the hardpan; and (iii) synchronisation of phenology amongst trees and grasses in the dry season. We propose that hydraulic redistribution provides a small amount of moisture that maintains functioning of the shallow roots during long periods when the surface soil layer was dry, thereby enabling Mulga to maintain physiological activity without diminishing phenological and physiological responses to precipitation when conditions were favourable to promote canopy cooling.

Keywords: *ecohydrology; resilience; soil moisture carry-over; climate extremes; semi-arid woodland; evergreen* Acacia

1 Introduction

The generic term *critical zone* was first used in 1909 to describe the chemical interface between two mixing fluids (Tsakalotos, 1909; cited from Lin, 2010), and more recently it has been used in petroleum geology (for mineral bearing strata of the Bushveld complex;

Ballhaus and Stumpfl, 1985), in cardiac physiology (Touboul *et al.*, 1992), and for the root–soil interface (Ryan *et al.*, 2001). Recently, the Earth's Critical Zone was defined to integrate the ecohydrology, climate and geology of the near-surface terrestrial environment, from the top of the vegetation through to the bottom of the aquifer (Lin, 2010; Banwart *et al.*, 2011; Chorover *et al.*, 2011; Lin, 2011). In this current paradigm, study of the Earth's Critical Zone often focuses on water as a unifying theme, through which soil moisture content (θ) is the medium that bridges biotic and abiotic processes by providing site memory and integrating climate and biological systems (Lin, 2010; Banwart *et al.*, 2011; Lin, 2011).

Vegetation dynamics (e.g., productivity) are primarily constrained by low soil moisture availability in dryland regions of the world, thus knowledge of the spatial and temporal dynamics of θ are crucial for understanding patterns and processes in dryland critical zones. Drylands include environments characterised by dry sub-humid, semi-arid, arid and hyper-arid climates, and their distribution covers 41% of global land area and is increasing (Reynolds *et al.*, 2007). θ in these regions is highly variable in space and time, where the physical, hydrologic and biotic characteristics of a given field site confer primary control of spatial variability in θ. For example, patchiness of infiltration can lead to variations in vertical and horizontal patterns of θ, nutrient redistribution, and biogeochemical weathering (Chorover *et al.*, 2011). Similarly, temporal variations in θ can be very strong in drylands, which experience pulses of precipitation interspersed by long dry periods (Huxman *et al.*, 2004b; Schwinning and Sala, 2004; Morton *et al.*, 2011). The dynamics of these pulses have an important impact on carbon assimilation by plants, which depend upon the amount, intermittency and magnitude of precipitation events (Porporato *et al.*, 2004). The trigger-transfer-reserve-pulse framework was developed to characterise ecohydrologic responses to rainfall intermittency in semi-arid landscapes (Ludwig *et al.*, 2005). In this framework, pulses of production by vegetation are triggered by pulses of precipitation that exceed a threshold for activity, which can be influenced by the amount of moisture already stored in the soil and by the transfer of water horizontally and vertically.

The water budget represents the balance between moisture input as precipitation (P) and output as evapotranspiration (ET), net runoff (Q, runoff − run-on), net drainage below the root zone (D, the difference between groundwater recharge and discharge) and the change in storage of θ ($\Delta\theta$):

$$P = ET + Q + D + \Delta\theta. \quad (1)$$

Much of the Australian drylands are covered by Mulga (*Acacia* spp.) shrubs and trees (30–35% of the semi-arid land area) (Bowman *et al.*, 2008), and these Mulga lands tend to be flat with negligible runoff or drainage (Pressland, 1976a; Murphy *et al.*, 2010; Moreno-de las Heras *et al.*, 2012; Chen *et al.*, 2014). Thus, slope and lithology alone explain 16% of Mulga distribution such that their density declines rapidly when the slope of the terrain increases above 2% (Murphy *et al.*, 2010). Furthermore, Mulga is distributed on water-storing substrates (sand dunes, clay-rich soils, and over hardpan) where drainage is limited or absent (Pressland, 1976a). As a potentially important source of water for maintaining physiological activity during dry seasons and droughts, the carry-over of stored soil moisture can influence phenology, productivity and ET (Flanagan and Adkinson, 2011; Chen *et al.*, 2016). Vegetation patches enhance infiltration by creating preferential flow paths along live and recently deceased roots and by concentrating delivery of water from precipitation to the base of the tree via stemflow (Ludwig *et al.*, 2005). Large proportions of precipitation (18–40%) are channelled as stemflow down the mostly vertical branches of Mulga, thereby concentrating the storage of soil moisture into a small area near the bole (Pressland, 1973, 1976b; Tongway and Ludwig, 1990). By concentrating rainfall to near the base of the trees, θ in the inter-tree spaces tends to be small even following precipitation, except following large storms (e.g., when the single-storm precipitation is larger than 50 mm; Pressland, 1976a). Local capture of soil moisture by Mulga contributes to disruption of runoff at the landscape scale but enhances local redistribution of moisture from open spaces to underneath the trees (Dunkerley and Brown, 1995). In Mulga where soil moisture storage capacity is large, understanding pulse responses alone is insufficient for understanding ecosystem responses to precipitation (Lauenroth *et al.*, 2014) because the reserve of soil moisture provides an important connection between a previous precipitation event and growth (Ludwig *et al.*, 2005).

The presence of a hardpan is an important feature of many semi-arid environments, having the potential for affecting local (i.e., fine scale) distributions of moisture availability (Mohawesh *et al.*, 2008). Various forms of siliceous (i.e., silica- or sand-based) hardpan underlie vast portions of the semi-arid regions of Australia (Litchfield and Mabbutt, 1962; Chartres, 1985), isolating the root zone from distant bedrock or groundwater in the locations

where it occurs (Cleverly *et al.*, 2016b). The physical characteristics of these hardpans have an important impact on the hydrology and ecology of the ecosystems where they occur. Siliceous hardpans form in dry sands containing traces of gypsum, opal and alunite (Thiry *et al.*, 2006). However, these binding agents dissolve when soil is wetted, and the durability of the hardpan (i.e., resistance to dissolution and infiltration) is proportional to the clay content of the soil (Litchfield and Mabbutt, 1962; Chartres, 1985). Thus, hardpans do not form in drainage sands, but they can underlie sand plains and dunes, creating an impenetrable barrier of varying thickness and depth and promoting accumulation of soil moisture in the unconsolidated soil above the hardpan. Hardpans in the strongly weathered red earths (kandosols) of Australia can be deep (> 3 m to the top of the hardpan), but large areas of the continent exist over a shallow hardpan buried between 0.3 and 1 m below the surface (Morton *et al.*, 2011). Because of this variation, siliceous hardpans could have a profound effect on local hydrology and θ. In landscapes containing a hardpan barrier to drainage, the total capacity for storage of water above the hardpan as soil moisture is proportional to the depth of unconsolidated soil above the hardpan. Thus, variability in hardpan depth is likely to affect plant and root distribution, which will then reinforce spatial patterns in θ. Consequently, Mulga density increases where depth to the top of the hardpan is large (Tongway and Ludwig, 1990), implying that Mulga density increases with soil moisture storage capacity above the hardpan. In this study, we will only address the fine-scale, not regional, effects of the hardpan on the relationships amongst θ, soil moisture storage, phenology and productivity.

Hydraulic redistribution by plant roots is found commonly in semi-arid regions, although it is not confined to drylands (Caldwell *et al.*, 1998). With hydraulic redistribution (of which "hydraulic lift" represents upward hydraulic redistribution), moisture is passively transported via roots across water potential gradients in the soil that are larger than the soil–leaf gradient (Hultine *et al.*, 2003a; Loik *et al.*, 2004; Neumann and Cardon, 2012). Reduction of the soil–leaf gradient in water potential is dependent upon substantial reductions in stomatal conductance and transpiration (Caldwell *et al.*, 1998; Hultine *et al.*, 2003b; Hultine *et al.*, 2004; Prieto *et al.*, 2010). Stomatal closure is known to occur at night (Caldwell and Richards, 1989; Hultine *et al.*, 2003b), during the dormant season (Hultine *et al.*, 2004) and during the day when atmospheric demand (i.e., vapour pressure deficit) is large (Zeppel *et al.*, 2004; Neumann and Cardon, 2012), as is the case in Mulga during drier-than-average periods

144 (Cleverly *et al.*, 2013a; Eamus *et al.*, 2013). Hydraulic redistribution (whether nocturnal,
145 dormant season or during daytime) can prevent root shrinkage (thereby maintaining contact
146 between root and soil), prevent loss of xylem conductivity and increase root longevity, even
147 into the dry season (Bauerle *et al.*, 2008; Scott *et al.*, 2008; Prieto and Ryel, 2014). By
148 maintaining root function during dry periods, some species have the potential to respond
149 rapidly following precipitation events without having to develop new root tissue.

150 Photosynthetic production in Mulga woodlands is driven by phenological responses in leaf-
151 level productivity, photosynthetic capacity and new leaf growth that are induced by pulses of
152 precipitation, which is why the enhanced vegetation index (EVI) is closely related to gross
153 primary production across Australian drylands (Ma *et al.*, 2013). Using the normalised
154 difference vegetation index (NDVI) from MODIS, Moreno-de las Heras *et al.* (2012) found
155 greenness in undisturbed Mulga to lag behind rainfall by 0–10 days at a given site (i.e., a lag
156 of zero to two 8-day scenes). Typically in ecosystems driven by precipitation pulses, a pulse
157 in net ecosystem productivity (NEP) follows precipitation by several days if the threshold for
158 activity has been met (Huxman *et al.*, 2004b), although the time required for photosynthetic
159 assimilation to initiate might be only one day, depending upon the plant species (Huxman *et*
160 *al.*, 2004a). NEP represents the integrated effects of phenology and productivity in all types
161 of photosynthetic organisms that are present in the ecosystem, thus the timing and magnitude
162 of a response in NEP could be shortened by differential responses to precipitation events
163 amongst organisms. Because of the close relationships between phenology and physiology,
164 Migliavacca *et al.* (2015) introduced the term *physiological phenology* to include the seasonal
165 variation in plant- and ecosystem-scale physiology (e.g., NEP).

166 Located where soils have a large capacity for storage of water, and the storms to recharge θ
167 are large and infrequent, Mulga is distributed in the more productive parts of the landscape
168 (Murphy *et al.*, 2010), where carbon is sequestered over long periods in woody tissue and
169 long-lived evergreen leaves/phyllodes (Morton *et al.*, 2011). An example of Mulga's
170 productiveness was the large responses of NEP and gross primary production in this Mulga
171 woodland to precipitation in 2011 (Cleverly *et al.*, 2013a; Eamus *et al.*, 2013). Mulga
172 rangelands were identified as one of the semi-arid ecosystems in Australia that together
173 contributed a majority (57%) of the 2011 global land carbon sink anomaly (Cleverly *et al.*,
174 2016a), which was an anomalous increase in terrestrial carbon uptake in response to

175 precipitation extremes across the Southern Hemisphere and associated reductions in mean sea
176 level (Boening *et al.*, 2012; Fasullo *et al.*, 2013) that impacted the global carbon cycle
177 (Poulter *et al.*, 2014). By contrast, during the drought year following 2011, the Mulga
178 woodlands were carbon neutral (i.e., NEP ≈ 0; Cleverly *et al.*, 2013a).

179 In this study, we evaluated the vertical, horizontal and temporal relationships between soil
180 moisture, leaf phenology and NEP in a semi-arid Mulga woodland of central Australia. The
181 primary photosynthetic organisms in this Mulga woodland are C_3 trees, an understorey
182 dominated by C_4 grasses, and biological soil crusts. The objective of this study was to
183 investigate relationships amongst soil moisture, NEP (i.e., ecosystem scale physiological
184 phenology), and phenological responses to precipitation in the photosynthetic organisms
185 comprising the ecosystem (i.e., trees, grasses and biological soil crusts). We compared
186 measurements of leaf greenness, NEP, θ and root distribution in a Mulga woodland to
187 investigate their relationships to key factors of the local water budget: precipitation and
188 storage of water in the soil ($\Delta\theta$). These measurements were collected locally at a fine scale to
189 test the following three hypotheses regarding the critical zone of this Mulga woodland:

190 1. Responses of NEP to precipitation (i.e., ecosystem-scale physiological phenology)
191 were expected to be proportional to inter-seasonal carry-over of stored soil moisture
192 above the top of the hardpan.

193 2. The responses of phenology in the component organisms (Mulga, understorey grasses
194 and biological soil crust) were hypothesised to respond differently to precipitation
195 such that soil crust was expected to respond immediately, whereas Mulga and
196 understorey grasses were hypothesised to respond more slowly with the growth of new
197 roots and leaves.

198 3. The rhizosphere was hypothesised to be restricted to the unconsolidated soil above the
199 hardpan (i.e., root density was hypothesised to be significantly larger above the
200 hardpan than in the top of the hardpan), which hypothetically forms a barrier for root
201 growth and infiltration of water, thereby also restricting soil moisture storage pools to
202 above the hardpan.

203

2 Methods

2.1 Study site

This study was conducted at the Alice Mulga SuperSite, a part of the OzFlux and Australian SuperSite networks. Complete descriptions of the vegetation and soils can be found in Eamus *et al.* (2013) and Cleverly *et al.* (2013b). Briefly, the site contains a high-density Mulga woodland (76% cover, 8 m^2 ha^{-1} basal area, 0.3–0.9 leaf area index) consisting of *Acacia aneura* and *A. aptaneura* (Eamus *et al.*, 2013; Cleverly *et al.*, 2016b). The extensive but sparse canopy results in very little shading of the understorey or soil by the canopy, thus the woodland is not dense enough, nor is the 6.5 m tall canopy tall enough, for this ecosystem to be considered a forest. The physiological activity of a seasonal understorey of tussock grasses (annual and perennial, C_3 and C_4, but largely C_4), forbs and shrubs is conditional upon receipt of adequate rainfall. The site also contains an extensive ground cover of biological soil crust, which consists primarily of cyanobacteria as the photosynthetic component (Jameson, 2012).

The location of this site is near the northern limit for Mulga, which is not found where winter precipitation is lacking, as is the case in the tropical savannas to the north (Nix and Austin, 1973). This site receives 86% of annual precipitation during the monsoon season between November and April (Cleverly *et al.*, 2013a), although this proportion varies inter-annually. The monsoon tropics of Australia are defined by receipt of at least 85% of annual precipitation in the monsoon season (Bowman *et al.*, 2010), which places the site just within the monsoon tropics. Average annual precipitation was 312.3 mm for the period 1987–November 2015 (http://www.bom.gov.au), with a range of 25.1 mm in 1928 to 954.9 mm in 1974 (SILO patched point data, https://www.longpaddock.qld.gov.au/silo/; Table 1).

The soil is loamy sand with an extensive siliceous hardpan. All of our measurements were made near the top of the hardpan or in the unconsolidated soil above the hardpan. We have inferred from soil moisture measurements (i.e., siliceous hardpans are dry with unvarying θ) that the top of the hardpan varies spatially, from the surface (i.e., surface expression of the hardpan; Cleverly *et al.*, 2013a) to more than one metre deep, which was the maximal depth at which we could insert soil moisture sensors into the highly compacted soil. The depth to the bottom of the hardpan is unknown, but possibly much deeper than could be excavated

(maximum of 2 m depth with the 1.5 tonne excavator to which we had access) in these hard, dense soils. Depth-to-groundwater is 49 m, and the site is located on the fringe of the regional aquifer where aquifer thickness is much smaller than 10 m (www.lrm.nt.gov.au/__data/assets/pdf_file/0003/13863/TiTree_Basin_Groundwater.pdf). The groundwater is too deep to affect the vegetation or water budget, even in the absence of the hardpan. In a carbon isotope ratio study of water-use efficiency, we inferred that the presence of a hardpan served as a barrier to groundwater access by vegetation, regardless of the depth to groundwater (8 or 49 m deep; Cleverly *et al.*, 2016b). Soil bulk density ranges from 0.9 to 2.1 g cm^{-3} in unconsolidated soil and hardpan, respectively.

2.2 Eddy covariance

The eddy covariance method (Baldocchi *et al.*, 1988) was used to measure NEP and sensible heat flux (H), the latter of which is which is indicative of partitioning of energy across seasons and years. Details on methods of measurements, quality control, corrections and gap filling can be found in Eamus *et al.* (2013) and Cleverly *et al.* (2013a). We will briefly summarise these methods here. These data are made available by the OzFlux network (Cleverly, 2011). Data processing was performed in the OzFluxQC Simulator, version 2.8.6 (Cleverly and Isaac, 2015), a summary of which follows.

NEP ($mgCO_2\ m^{-2}\ s^{-1}$) and H ($W\ m^{-2}$) were determined as the negative covariance between vertical wind speed (w) *versus* CO_2 density (c) or air temperature (T), respectively:

$$NEP = -\rho\left\langle w'c'\right\rangle \text{ and} \qquad 2$$

$$H = \rho C_p\left\langle w'T'\right\rangle. \qquad 3$$

where ρ and C_p are the density and heat capacity of moist air, respectively; w', c' and T' are the deviations from mean w and c and T, respectively; and $\langle\ \rangle$ represents a time average. Measurements were collected at 10 Hz, and the averaging period was 30 minutes. Measurements were made at a height of 11.7 m over the homogeneous 6.5 m tall canopy. Wind speed measurements were made in three dimensions using a CSAT3 sonic anemometer (Campbell Scientific Australia, Townsville, QLD, Australia), and CO_2 density measurements were obtained from a LI7500 infrared gas analyser (IRGA, Li-Cor Biosciences, Lincoln, NE,

USA). Ancillary measurements collected by the eddy covariance system were used in the subsequent quality control procedures and included precipitation (CS7000, Hydrologic services, Warwick, NSW, Australia); temperature and relative humidity (HMP45C, Vaisala, Helsinki, Finland); and radiant fluxes in four components: upwelling and downwelling solar and thermal radiation (CNR1, Kipp and Zonen, Delft, The Netherlands). The system also included measurements of temperature and relative humidity (HMP45C) in a profile at heights of 2 m, 4.25 m (the zero-plane displacement height) and 6.5 m (the average canopy height) (Cleverly *et al.*, 2013b).

2.2.1 Quality control, corrections and gap filling

Standard QC methods included spike detection using a standard deviation test, range checks for unrealistic values, identification of invalid measurements form CSAT and IRGA diagnostics, and identification of invalid IRGA measurements from outliers in the relationship between humidity measured by the HMP45C and IRGA. Corrections included double rotation, the Massman frequency response correction, conversion of virtual heat flux to sensible heat flux, and the Webb-Pearman-Leuning correction for flux effects on density measurements (Wesely, 1970; Webb *et al.*, 1980; Massman and Clement, 2004). When there were no gaps in the ancillary measurements, gap filling of fluxes was performed using a self-organising linear output (SOLO) model, which is a type of artificial neural network (ANN) that produces small errors and has low sensitivity to overtraining, in contrast to feed-forward ANNs (Hsu *et al.*, 2002; Eamus *et al.*, 2013).

2.3 Phenocams and airborne imagery

Images of the vegetation (understorey grasses, Mulga canopy) and cryptobiotic crust were collected hourly during the daytime for evaluation of phenological activity. The cameras (5 Megapixel Wingscape timelapse, Wingscapes, AL, USA) were designed for repeat photography and configured to maintain a fixed white balance. The cameras were positioned at a 30° inclination and facing North to avoid backscattering during most of the year. Images that were obtained near solar noon were analysed for the green:red ratio index (GRRI), which provides an index of "greenness" that represents the trade-off between photosynthesis (due to chlorophyll content) and thermal dissipation (due to anthocyanin content) (Gamon and Surfus, 1999; Ritchie *et al.*, 2010). Within each image, pixels were classified as Mulga, grass, crust

or soil, after which GRRI was determined using Matlab (R2013a, The MathWorks Inc., Natick Massachusetts USA). Larger values of GRRI are indicative of enhanced physiological capacity. Because of technical issues with powering the cameras, analysis of phenology was restricted to a few precipitation events during key seasons.

Radiometric canopy temperature was measured to evaluate the thermal environment of the Mulga within the context of its photosynthetic thermal tolerances (i.e., 30 °C thermal optimum and 38 °C limit for photosynthesis and growth; Nix and Austin, 1973). Because the radiometric temperature of understorey and crust elements is indistinguishable from soil temperature due to their proximity to this large source of heat, this analysis was focused upon the canopy trees (i.e., Mulga). This analysis will determine if Mulga's thermal environment is conducive for maintenance of phyllode function. Aerial imagery was obtained on 27 March 2014 from an unmanned aerial vehicle (UAV), the AT8 octocopter of AerialTronics (Scheveningen, The Netherlands). Imagery was captured near midday to minimise shadow effects. The camera gimbal was set at a vertical angle (nadir-looking) during the flights. Two cameras were on board the UAV: a digital camera (red, green and blue; RGB) and a thermal camera. The thermal camera was a FLIR SC305 (FLIR Systems, Inc., Wilsonville, OR, USA) with a resolution of 320×240 pixels, a thermal accuracy of ±2 °C, and a thermal sensitivity of 0.05 °C. The thermal field of view (FOV) was 45° × 34° (equipped with a 10 mm lens). All FLIR images were converted to canopy temperature tiff-images as described by Maes *et al.* (2014). Geo-referenced thermal and visual orthophotos were registered and co-registered manually in ArgGIS 10.1 (ESRI, Redlands, CA, USA).

2.4 Soil moisture and root profile characterisation

θ was measured in six arrays of vertical profiles. Sensors (CS616 and CS605) were buried at four depths: 0–10 cm (surface), 10–30 cm, 60–80 cm and 100–130 cm. These vertical profiles of θ measurements were obtained from two arrays within each of three key habitats: under Mulga, in bare soil between trees, and beneath both Mulga and understorey. The latter habitat was identified during the build-up of the 2011 land carbon sink anomaly, when the understorey of grasses and herbs was present (Eamus *et al.*, 2013). To avoid the confounding effects of transience of the understorey on patterns in θ, we will present profiles from beneath the canopy and inter-canopy bare soil only. Calibration of the sensors, which is necessary to

ensure accurate measurement of θ, was performed by comparison to soil samples for laboratory analysis of soil texture, bulk density and θ (Cleverly *et al.*, 2013a).

Six trenches were dug about 1.2 km to the east of the tower in the Mulga woodland for evaluation of root density profiles with depth. Because of the large fetch of relatively homogenous vegetation at the tower (> 10 km in the predominant wind directions; Cleverly *et al.*, 2013a), the location where the trenches were dug is representative of the ecosystem where continuous measurements of θ were collected. Furthermore, flux footprints can extend this far under stable conditions at night (Göckede et al., 2008), further implying that this location is representative of the tower site to the west. Trenches were placed in three habitats: beneath Mulga near the bole (Mulga), in bare soil patches (bare soil) and below the edge of the projected canopy. Intact soil cores were collected for root extraction from the trench face at 25 cm intervals to a depth of 125 cm. Additional soil cores for analysis of bulk density and θ were collected to identify the top of the hardpan. The hardpan varied spatially by habitat at the trench locations as it does in the soil moisture arrays at the tower. The top of the hardpan varied between 0 and 0.6 m deep, in contrast to the tower site where the top of the hardpan varied from the surface to more than one metre deep. The Mulga were shorter and less dense where the trenches were dug, thus facilitating access for the excavator. Roots were extracted from soil samples using a hydro-pneumatic elutriation system, in which a soil and root sample is submerged in a vertical column of flowing water, whilst the sample is agitated with low-pressure air (Smucker *et al.*, 1982). Hydro-pneumatic elutriation is the most reliable means to separate roots from soil. The null hypothesis that no differences in root density amongst sampling locations would be found was tested using a two-factor ANOVA (depth × habitat, $\alpha = 0.05$) followed by *post-hoc* multiple comparisons (Matlab R2013).

3 Results

3.1 Soil moisture control over phenological responses to precipitation

The balance between photosynthetic production and physiological stress is represented by the green:red ratio index (GRRI) of the vegetation, and this ratio varied by growth form and season in the current study (Fig. 1). During the spring and early summer, three surfaces (understorey grass, Mulga foliage and cryptobiotic crust) had distinct GRRI values, and the

larger GRRI for the grasses indicated that grasses were more active than Mulga, and both were greener than the crust (Fig. 1a). Immediate but unsustained greening responses to precipitation during the spring and early summer were evident in all surface types. By autumn, the three surface types had similar spectral responses to rainfall (Fig. 1b). However, inferences cannot be drawn during the intervening period because of equipment failure at this remote location.

Whereas the response of NEP to rainfall was delayed in January–March 2014, there was an immediate increase in NEP during January 2015 (Fig. 2b). Striking differences in the pattern of precipitation were present between these two summers. During January 2014, the single largest storm delivered 105 mm precipitation over six consecutive days. By contrast, 145 mm of precipitation fell over 12 consecutive days in January 2015. Even though each wet season received the same amount of precipitation, during the second year it was concentrated in December 2014 and January 2015 and was then followed by many months without substantial precipitation (Fig. 2b).

Differences in the pattern of precipitation during the wet season had a large effect on θ of the root zone (Fig. 3). In Summer–Autumn 2013–2014, θ in the unconsolidated soil above the hardpan increased to 0.26 m^3 m^{-3} and remained at that level during the six week delay in NEP (cf. Figs. 2a and 3a), whereas θ in the unconsolidated soil above the hardpan declined immediately during the next wet season (summer–autumn 2014–2015; Fig. 3b). Most of the year's precipitation was concentrated into a short period during December 2014–January 2015 (Figs. 2b and 3b), resulting in saturation of θ in the unconsolidated soil above the hardpan at one metre depth (Fig. 3b). Two-to-three weeks after saturation in the unconsolidated soil (mid-to-late January 2015), θ in the hardpan at one metre depth showed a slight increase, which was the first observed change in this very dry soil since measurements began in 2010.

Canopy temperature varied between a minimum of 33 °C and a maximum of 50 °C, although temperatures above *ca*. 46 °C were restricted to the edges of canopies (Fig. 4). Canopy temperatures were not uniformly distributed across the site, but it is difficult to identify a pattern in the clumped distribution of cool *versus* hot canopies. Canopy air temperature on the day of the thermal imagery was 25.1 °C at 10.00, 28.1 °C at 12.00 and reached a maximum of 31.4 °C at 16.30. Thus, radiometric canopy temperatures were all above ambient air temperature, even after accounting for the ±2 °C precision of the thermal camera.

Mid-day air temperatures tended to be lower in the seasons when NEP was large (autumn 2014 and summer 2015; cf. Table 2 and Fig. 2). Mid-day sensible heat flux was smallest during summer 2015, the wet season when NEP was large (cf. Table 2 and Fig. 2b). Sensible heat flux was equal in wet and dry seasons of 2014, although consistent season × year relationships emerged. During summer 2014 (when NEP was delayed relative to precipitation), sensible heat flux was larger than during summer 2015 (when the response of NEP to precipitation was immediate; cf. Table 2 and Fig. 2b). Similarly, sensible heat flux in autumn 2014 (when NEP was large) was smaller than during autumn 2015 (when NEP was declining; cf. Table 2 and Fig. 2a).

The θ profiles showed varied responses to precipitation (Fig. 5). Under dry conditions before summer rainfall, θ at the surface was small in both habitats and smaller in bare soil (0.031 ± 0.000074 m^3 m^{-3}) than under Mulga (0.054 ± 0.0012 m^3 m^{-3}; Fig. 5). In response to a small autumnal storm (30 mm), moisture penetrated no more than 10 cm into the soil (Fig. 5a, b). By contrast, a large storm (100+ mm) produced widely varying soil moisture dynamics (Fig. 5c). The wetting front did not reach to one metre depth in half of the profiles, whilst θ was very large beneath Mulga where the θ had been already large (i.e., in the consolidated soil above the hardpan; cf. Figs. 3a and 5c) and at one location beneath bare soil, implying that the durability of the hardpan against wetting was spatially variable.

3.2 Rhizosphere

Significant variation in root density was found within the woodland (depth × habitat $F = 6.09$; $df = 10, 287$; $p < 0.0001$). Substantial amounts of root biomass were observed only above 75 cm depth and directly beneath the base of Mulga trees. Root density in bare soil was not significantly different from root density at the edge of the canopy, regardless of depth (Fig. 6). Root density was significantly larger near the boles of Mulga trees than in bare soil or under the edge of the canopy at depths of 5 and 50 cm (Fig. 6). The largest amounts of root biomass were located in the top 10 cm, although a secondary proliferation of root biomass above the top of hardpan (*ca.* 60 cm depth at the base of the trees) was also evident (Fig. 6).

Figure 7 shows the daily soil moisture drawdown above the hardpan at 100 cm depth. During inter-storm periods, θ above the hardpan at 100 cm depth began declining between 10:00 and 11:00 (0.11 ± 0.00095 m^3 m^{-3}) and continued until reaching a minimum at 17:00 (0.083 ±

0.0017 m^3 m^{-3}; Fig. 7). Recovery of θ was rapid and reached the previous day's value before midnight (Fig. 7). In contrast during storms, diel variations in θ above the hardpan at 100 cm depth were negligible (i.e., smaller than the measurement error; Fig. 7). The preceding soil moisture and rhizosphere results are summarised in Figure 8.

4 Discussion

4.1 Triggers for photosynthetic responses

Reserves of soil moisture can serve as an important connection between precipitation and NEP (Ludwig *et al.*, 2005; Flanagan and Adkinson, 2011). As we hypothesised, the storage of soil water provided inter-seasonal carry-over of available moisture, thereby supporting the enhancement of NEP during autumn 2014 (March 2014) after the conclusion of the wet season (Fig. 2a). By contrast, soil moisture carry-over did not occur during the wet season of a drier-than-average year (2012–2013, θ *ca*. 0.10 m^3 m^{-3} in the unconsolidated soil above the hardpan), resulting in suppression of NEP through both summer and autumn (Cleverly *et al.*, 2016b). The delay of enhanced NEP in 2014 was related to the imposition of environmental stress in Mulga. For example, photosynthesis and transpiration in Mulga phyllodes can be limited by high temperature and large vapour pressure deficit during summertime inter-storm periods (Cleverly *et al.*, 2013a; Eamus *et al.*, 2013). Mid-day air temperatures remained relatively high into autumn (Table 1), leaving a substantial portion of the canopy above the thermal limit for Mulga (38 °C; Fig. 4). More importantly, enough of the canopy was much cooler (33–34 °C) than the thermal limit to suggest that modest amounts of soil moisture in storage (0.26 m^3 m^{-3}) provided an amount of water that was sufficient to prevent overheating of the canopy through evaporative cooling, but this amount wasn't sufficient until autumn.

When the soil moisture storage pool above the hardpan was filled to saturation in response to receiving large amounts of precipitation over several days (> 120 mm wk^{-1}), NEP increased immediately during the summer (i.e., completely filling soil moisture stores resulted in no delay in NEP). The threshold for vegetation activity across Australia can be much smaller than this (6 mm; Martin, 2006), although this low threshold is more likely associated with an ecosystem respiratory response alone (Huxman *et al.*, 2004b). Our results are consistent with the threshold-delay framework (Ogle and Reynolds, 2004), in which we identified two

443 threshold amounts of precipitation: one below 150 mm for inducing a delayed response in
444 NEP, and the other above 100 mm that induced a pulse response without a delay (cf. Figs. 2
445 and 3). The threshold for moving from a delayed NEP response to an immediate one suggests
446 that water, and more specifically θ in the storage pool above the hardpan, was the primary
447 agent determining the presence or absence of a delay.

448 Evapotranspiration can reduce canopy temperature in plants (Yunusa *et al.*, 2004), but this
449 mechanism is seldom considered with microphyllous vegetation because the large boundary
450 layer conductance of small leaves tends to keep them in thermal equilibrium with the air
451 (Schuepp, 1993). However, the boundary layer of the entire tree crown can be large, even in
452 trees with microphyllous leaves (Daudet *et al.*, 1999), thus evaporative cooling of canopy air
453 spaces can be found in ecosystems dominated by trees with small leaves (e.g., Cleverly *et al.*,
454 2015). Two relationships emerged from seasonal variations in air temperature, sensible heat
455 flux and NEP. First, sensible heat flux was smallest in the summer wet season, especially
456 when NEP was large (January–February 2015). In part, this unsurprising result occurred
457 because sensible heat flux is inversely proportional to latent heat flux, which is larger in the
458 wet season. However, there was no difference in sensible heat flux between summer and
459 autumn in the previous year, suggesting that air temperature and NEP affected the seasonal
460 progression of sensible heat fluxes. A second relationship was present between NEP and air
461 temperature in which the season within a given year when NEP was large also experienced
462 cooler temperatures (Table 2). This does not imply that there is a causative relationship
463 between NEP and air temperature because there are other meteorological factors that might
464 distinguish these two years. Nonetheless, saturation of soil moisture reserves created a
465 temporary perched aquifer above the hardpan, and this could have provided sufficient
466 resources to generate evaporative cooling of the canopy and promote photosynthesis (and thus
467 positive NEP) during the summertime, thus reducing canopy air temperature. Evaporative
468 cooling inferred in our study is not equivalent to the intense evaporative cooling that is
469 observed in groundwater-dependent ecosystems and irrigated agriculture (Stevens *et al.*,
470 2012; Cleverly *et al.*, 2015), but it is conceivably enough to reduce thermal stress in within
471 the canopy.

472 We found very few differences in phenological responses to precipitation amongst trees,
473 understorey grasses and biological soil crusts, thus rejecting our hypothesis that differential

474 constraints on photosynthesis in these different types of organisms would lead to divergent
475 phenological patterns. The limited collection of phenocam imagery was not ideal, having
476 been collected during a drier-than-average year (summer 2012–2013) when minimal NEP was
477 in evidence (Cleverly *et al.*, 2016b), but the phenological patterns that we observed can still
478 inform us about the potential of each component of the ecosystem to contribute to NEP. The
479 small values of GRRI for the soil crust in spring–early summer suggest that photosynthesis is
480 constrained during summer, which was probably due to the effect of high temperature (Grote
481 *et al.*, 2010). In contrast, photosynthesis in the C_4 understorey grasses should not be limited
482 by high temperature because of their resistance to photorespiration (Ehleringer *et al.*, 1991;
483 Ehleringer and Monson, 1993). Instead, the phenology of grasses matched that of Mulga
484 (Fig. 1), which suggests that both contributed to the delay in NEP during the summer of 2014.
485 The delay in the phenology of the grasses was surprising because rainfall amounts were large
486 enough during January and February 2014 to expect a growth of understorey grasses. Either
487 some other factor was related to phenology in both types of vegetation, or the understorey
488 grasses were facilitated by physiological activity in Mulga.

489 ## 4.2 Supporting the survival of a largely shallow root system

490 Mulga root systems are dimorphic, and we found them to be mostly restricted to above the
491 hardpan in the unconsolidated soil as hypothesised, but the largest biomass was found near
492 the surface (Fig. 5). The surface soil dries rapidly in this loamy sand (Eamus *et al.*, 2013),
493 thereby having a potentially detrimental effect on the roots located near the surface. A second
494 and smaller proliferation of root biomass was located just above the top of the hardpan in the
495 unconsolidated soil where storage of moisture accumulates. θ in this store above the hardpan
496 is drawn down by more than 0.02 m^3 m^{-3} on days without precipitation, although there are no
497 discharge points for this soil moisture: evapotranspiration was at a minimum (Cleverly *et al.*,
498 2016b), and drainage into the hardpan below was generally negligible. Furthermore,
499 drawdown of θ above the hardpan occurred during the hottest part of the day (Fig. 7), when
500 Mulga are known to experience suppression of assimilation and stomatal conductance (Eamus
501 *et al.*, 2013) and when temperatures exceed the thermal tolerances for Mulga (Fig. 4; Cleverly
502 *et al.*, 2013a).

503 Stomatal closure in the presence of a split root system in which some roots are in dry soil and
504 others are in wet soil presents the possibility of hydraulic lift (Bauerle *et al.*, 2008). In this
505 case, hydraulic redistribution would travel from roots in the soil moisture store above the
506 hardpan to roots near the surface. Although we were unable to confirm the following
507 reasoning with sapflux measurements, there are three lines of indirect evidence to support this
508 hypothesis. First, the absence of discharge by evapotranspiration or drainage accounts for the
509 other terms of the water budget; therefore, fluctuations in θ were due to internal cycling (i.e.,
510 local changes in soil moisture storage). Second, we found a large proportion of the root
511 biomass to occur near the surface where θ is much smaller than at depth (Fig. 6), which is not
512 unusual *per se*, except when encountered in dry soil (Caldwell *et al.*, 1998). Third,
513 synchronisation of tree and grass phenology after a delay in NEP further implies that the
514 shallow-rooted tussock grasses obtain soil moisture as a result of moistening of the surface
515 soil by hydraulic lift (Pugnaire *et al.*, 1996; Ludwig *et al.*, 2003), particularly in the absence
516 of other soil moisture sources. During the delay period, high canopy temperature and
517 unsaturated θ kept the effects of hydraulic lift to a minimum, and precipitation alone was
518 insufficient to sustain the understorey grasses. In the absence of other discharge points for
519 soil moisture drawdown in the reservoir above the hardpan, it was most likely that hydraulic
520 lift provided the connection between the synchronised phenology of individual photosynthetic
521 organisms (trees, grasses and biological soil crust) and NEP.

522 Drawdown of θ above the hardpan did not occur during storms, regardless of the amount of
523 precipitation that was received. However, drawdown then resumed immediately upon the end
524 of precipitation events (Fig. 7). This cessation of hydraulic lift is in contrast to a previous
525 study on *Eucalyptus camaldulensis* and *Grevillea robusta* in which the seasonal return of
526 rainfall initiated a reversal of hydraulic redistribution (i.e., translocation of soil moisture to
527 deeper, drier soil layers; Burgess *et al.*, 1998). There are two conditions during stormy
528 periods that would tend to suppress, rather than reverse, hydraulic redistribution: (i) if
529 precipitation wets the surface soils to equivalent θ as in the soil moisture reserve, thereby
530 eliminating or substantially reducing gradients in soil water potential (Hultine *et al.*, 2003b);
531 or (ii) if plant water status is much improved under small vapour pressure deficit during
532 precipitation and cloud cover (Cleverly *et al.*, 2013a; Page *et al.*, 2016), resulting in small but
533 non-negligible rates of stomatal conductance throughout the day. Thus, the water potential

gradient during stormy conditions from any part of the root system to the air *via* stomata was much larger than water potential gradients across the root system, thereby eliminating the conditions favourable for hydraulic redistribution and resulting in cessation of daily fluctuations in θ.

5 Conclusions

Covering 20–25% of Australia, Mulga woodlands are a potentially important part of continental carbon and water dynamics. The persistence and responsiveness of these woodlands can be understood through a detailed understanding of the critical zone, and particularly those attributes of the lithoshpere, hydrosphere, biosphere and atmosphere that interact to drive constraints on the growth and productivity of vegetation. In north central Australia, the presence of siliceous hardpan can influence the spatial distribution of soil moisture reservoirs and roots within a few metres of the surface. These soil moisture reservoirs above the hardpan provide for the carry-over of soil moisture within the shallow rhizosphere of Mulga across seasons and years.

Carry-over of soil moisture can be a crucial resource for vegetation that experiences prolonged dry periods. In semi-arid regions, recharge of soil moisture reservoirs can be unpredictable, as can the duration between recharge events. It is common for precipitation to fail in central Australia, but the conservative use of soil moisture imposed by thermal stress on the canopy as the reservoir is drained ensures that carry-over persists beyond a single year. Even upon receiving large amounts of precipitation (100 mm wk^{-1}), the accumulation of soil moisture provides a buffer for delaying productivity until favourable conditions are present, when evaporation of that moisture contributes to preventing overheating of the canopy above Mulga's thermal limit.

Mulga has a dimorphic root distribution, with the majority of the root biomass in the top 10 cm of the soil and a second significant proliferation of roots just above the hardpan. During the long, dry periods between storms, the presence of hydraulic lift to the shallow roots was inferred from daily fluctuations in θ above the hardpan, synchronisation of phenology amongst grasses and trees, and the absence of other discharge points (i.e., negligible drainage and evapotranspiration). We propose that through this mechanism, functioning of the shallow

root system was maintained, which provided Mulga's roots and evergreen leaves with the capability of responding rapidly (i.e., if the conditions were favourable) to short, unpredictable, and large storms (i.e., with immediate moisture uptake through the roots to support immediate photosynthetic responses in the leaves). This resilience (i.e., physiological drought tolerance that does not diminish photosynthetic responses to subsequent wet periods) is the fundamental property that placed the Mulga lands of Australia in the heart of the 2011 global land carbon sink anomaly.

Acknowledgements

This work was supported by grants from the Australian Government's Terrestrial Ecosystems Research Network (TERN) (www.tern.gov.au), the National Centre for Groundwater Research and Training (NCGRT), and the Australian Research Council. This work was supported also by OzFlux and the Australian Supersite Network, both parts of TERN and the latter of which is a research infrastructure facility established under the National Collaborative Research Infrastructure Strategy and Education Infrastructure Fund, Super Science Initiative, through the Department of Industry, Innovation, Science, Research and Tertiary Education. This research as also supported by a UTS re-establishment grant to "setup a phenocam network on key Australian ecosystems."

583 **References**

584 Baldocchi DD, Hicks BB, Meyers TP. 1988. Measuring biosphere-atmosphere exchanges of
585 biologically related gases with micrometeorological methods. *Ecology* **69**:1331-1340.

586 Ballhaus CG, Stumpfl EF. 1985. Occurrence and petrological significance of graphite in the
587 upper critical zone, Western Bushveld complex, South Africa. *Earth and Planetary*
588 *Science Letters* **74**:58-68. DOI: 10.1016/0012-821x(85)90166-9.

589 Banwart S, Bernasconi SM, Bloem J, Blum W, Brandao M, Brantley S, Chabaux F, Duffy C,
590 Kram P, Lair G, Lundin L, Nikolaidis N, Novak M, Panagos P, Ragnarsdottir KV,
591 Reynolds B, Rousseva S, de Ruiter P, van Gaans P, van Riemsdijk W, White T, Zhang
592 B. 2011. Soil Processes and Functions in Critical Zone Observatories: Hypotheses and
593 Experimental Design. *Vadose Zone Journal* **10**:974-987. DOI: 10.2136/vzj2010.0136.

594 Bauerle TL, Richards JH, Smart DR, Eissenstat DM. 2008. Importance of internal hydraulic
595 redistribution for prolonging the lifespan of roots in dry soil. *Plant Cell and*
596 *Environment* **31**:177-186. DOI: 10.1111/j.1365-3040.2007.01749.x.

597 Boening C, Willis JK, Landerer FW, Nerem RS, Fasullo J. 2012. The 2011 La Niña: So
598 strong, the oceans fell. *Geophysical Research Letters* **39**. DOI:
599 10.1029/2012gl053055.

600 Bowman D, Boggs GS, Prior LD. 2008. Fire maintains an *Acacia aneura* shrubland—*Triodia*
601 grassland mosaic in central Australia. *Journal of Arid Environments* **72**:34–47. DOI:
602 10.1016/j.jaridenv.2007.04.001.

603 Bowman D, Brown GK, Braby MF, Brown JR, Cook LG, Crisp MD, Ford F, Haberle S,
604 Hughes J, Isagi Y, Joseph L, McBride J, Nelson G, Ladiges PY. 2010. Biogeography
605 of the Australian monsoon tropics. *Journal of Biogeography* **37**:201–216. DOI:
606 10.1111/j.1365-2699.2009.02210.x.

607 Burgess SSO, Adams MA, Turner NC, Ong CK. 1998. The redistribution of soil water by tree
608 root systems. *Oecologia* **115**:306-311. DOI: 10.1007/s004420050521.

609 Caldwell MM, Dawson TE, Richards JH. 1998. Hydraulic lift: Consequences of water efflux
610 from the roots of plants. *Oecologia* **113**:151-161. DOI: 10.1007/s004420050363.

611 Caldwell MM, Richards JH. 1989. Hydraulic lift: water efflux from upper roots improves
612 effectiveness of water uptake by deep roots. *Oecologia* **79**:1-5. DOI:
613 10.1007/bf00378231.

614 Chartres CJ. 1985. A preliminary investigation of hardpan horizons in Northwest New South
615 Wales. *Australian Journal of Soil Research* **23**:325-337. DOI: 10.1071/sr9850325.

616 Chen C, Cleverly J, Zhang L, Yu Q, Eamus D. 2016. Modelling seasonal and inter-annual
617 variations in carbon and water fluxes in an arid-zone *Acacia* savanna woodland, 1981–
618 2012. *Ecosystems* **19**:625–644. DOI: 10.1007/s10021-015-9956-8.

619 Chen C, Eamus D, Cleverly J, Boulain N, Cook P, Zhang L, Cheng L, Yu Q. 2014. Modelling
620 vegetation water-use and groundwater recharge as affected by climate variability in an
621 arid-zone *Acacia* savanna woodland. *Journal of Hydrology* **519**:1084–1096. DOI:
622 10.1016/j.jhydrol.2014.08.032.

623 Chorover J, Troch PA, Rasmussen C, Brooks PD, Pelletier JD, Breshears DD, Huxman TE,
624 Kurc SA, Lohse KA, McIntosh JC, Meixner T, Schaap MG, Litvak ME, Perdrial J,
625 Harpold A, Durcik M. 2011. How water, carbon, and energy drive critical zone
626 evolution: The Jemez-Santa Catalina Critical Zone Observatory. *Vadose Zone Journal*
627 **10**:884-899. DOI: 10.2136/vzj2010.0132.

628 Cleverly J. 2011. Alice Springs Mulga OzFlux site. OzFlux: Australian and New Zealand
629 Flux Research and Monitoring Network, hdl.handle.net/102.100.100/8697.

630 Cleverly J, Boulain N, Villalobos-Vega R, Grant N, Faux R, Wood C, Cook PG, Yu Q, Leigh
631 A, Eamus D. 2013a. Dynamics of component carbon fluxes in a semi-arid *Acacia*
632 woodland, central Australia. *Journal of Geophysical Research-Biogeosciences*
633 **118**:1168–1185. DOI: 10.1002/jgrg.20101.

634 Cleverly J, Chen C, Boulain N, Villalobos-Vega R, Faux R, Grant N, Yu Q, Eamus D. 2013b.
635 Aerodynamic resistance and Penman-Monteith evapotranspiration over a seasonally
636 two-layered canopy in semiarid central Australia. *Journal of Hydrometeorology*
637 **14**:1562–1570. DOI: 10.1175/jhm-d-13-080.1.

638 Cleverly J, Eamus D, Luo Q, Restrepo Coupe N, Kljun N, Ma X, Ewenz C, Li L, Yu Q, Huete
639 A. 2016a. The importance of interacting climate modes on Australia's contribution to
640 global carbon cycle extremes. *Scientific Reports* **6**:23113. DOI: 10.1038/srep23113.

641 Cleverly J, Eamus D, Van Gorsel E, Chen C, Rumman R, Luo Q, Restrepo Coupe N, Li L,
642 Kljun N, Faux R, Yu Q, Huete A. 2016b. Productivity and evapotranspiration of two
643 contrasting semiarid ecosystems following the 2011 global carbon land sink anomaly.
644 *Agricultural and Forest Meteorology* **220**:151-159. DOI:
645 10.1016/j.agrformet.2016.01.086.

646 Cleverly J, Isaac P. 2015. *OzFluxQC Simulator version 2.8.6*. GitHub repository,
647 github.com/james-cleverly/OzFluxQC_Simulator. DOI: 10.5281/zenodo.13730.

648 Cleverly J, Thibault JR, Teet SB, Tashjian P, Hipps LE, Dahm CN, Eamus D. 2015. Flooding
649 regime impacts on radiation, evapotranspiration and latent heat fluxes over
650 groundwater-dependent riparian cottonwood and saltcedar forests. *Advances in*
651 *Meteorology* **2015**:935060. DOI: 10.1155/2015/935060.

652 Daudet FA, Le Roux X, Sinoquet H, Adam B. 1999. Wind speed and leaf boundary layer
653 conductance variation within tree crown - Consequences on leaf-to-atmosphere
654 coupling and tree functions. *Agricultural and Forest Meteorology* **97**:171-185. DOI:
655 10.1016/s0168-1923(99)00079-9.

656 Dunkerley DL, Brown KJ. 1995. Runoff and runon areas in a patterned chenopod shrubland,
657 arid western New South Wales, Australia — characteristics and origin. *Journal of Arid*
658 *Environments* **30**:41-55.

659 Eamus D, Cleverly J, Boulain N, Grant N, Faux R, Villalobos-Vega R. 2013. Carbon and
660 water fluxes in an arid-zone *Acacia* savanna woodland: An analyses of seasonal
661 patterns and responses to rainfall events. *Agricultural and Forest Meteorology* **182–**
662 **183**:225–238. DOI: 10.1016/j.agrformet.2013.04.020.

663 Ehleringer JR, Monson RK. 1993. Evolutionary and ecological aspects of photosynthetic
664 pathway variation. *Annual Review of Ecological Systematics* **24**:411-439.

665 Ehleringer JR, Sage RF, Flanagan LB, Pearcy RW. 1991. Climate change and the evolution of
666 C_4 photosynthesis. *Trends in Ecology & Evolution* **6**:95-99. DOI: 10.1016/0169-
667 5347(91)90183-x.

668 Fasullo JT, Boening C, Landerer FW, Nerem RS. 2013. Australia's unique influence on global
669 sea level in 2010-2011. *Geophysical Research Letters* **40**:4368-4373. DOI:
670 10.1002/grl.50834.

671 Flanagan LB, Adkinson AC. 2011. Interacting controls on productivity in a northern Great
672 Plains grassland and implications for response to ENSO events. *Global Change*
673 *Biology* **17**:3293–3311. DOI: 10.1111/j.1365-2486.2011.02461.x.

674 Gamon JA, Surfus JS. 1999. Assessing leaf pigment content and activity with a reflectometer.
675 *New Phytologist* **143**:105-117. DOI: 10.1046/j.1469-8137.1999.00424.x.

676 Göckede M, Foken T, Aubinet M, Aurela M, Banza J, Bernhofer C, Bonnefond JM, Brunet
677 Y, Carrara A, Clement R, Dellwik E, Elbers J, Eugster W, Fuhrer J, Granier A,
678 Grunwald T, Heinesch B, Janssens IA, Knohl A, Koeble R, Laurila T, Longdoz B,
679 Manca G, Marek M, Markkanen T, Mateus J, Matteucci G, Mauder M, Migliavacca
680 M, Minerbi S, Moncrieff J, Montagnani L, Moors E, Ourcival JM, Papale D, Pereira J,
681 Pilegaard K, Pita G, Rambal S, Rebmann C, Rodrigues A, Rotenberg E, Sanz MJ,
682 Sedlak P, Seufert G, Siebicke L, Soussana JF, Valentini R, Vesala T, Verbeeck H,
683 Yakir D. 2008. Quality control of CarboEurope flux data - Part 1: Coupling footprint
684 analyses with flux data quality assessment to evaluate sites in forest ecosystems.
685 *Biogeosciences* **5**:433-450.

686 Grote EE, Belnap J, Housman DC, Sparks JP. 2010. Carbon exchange in biological soil crust
687 communities under differential temperatures and soil water contents: implications for
688 global change. *Global Change Biology* **16**:2763-2774. DOI: 10.1111/j.1365-
689 2486.2010.02201.x.

690 Hsu K-l, Gupta HV, Gao X, Sorooshian S, Imam B. 2002. Self-organizing linear output map
691 (SOLO): An artificial neural network suitable for hydrologic modeling and analysis.
692 *Water Resources Research* **38**:1302. DOI: 10.1029/2001wr000795.

693 Hultine K, Cable W, Burgess S, Williams D. 2003a. Hydraulic redistribution by deep roots of
694 a Chihuahuan Desert phreatophyte. *Tree Physiology* **23**:353-360.

695 Hultine KR, Scott RL, Cable WL, Goodrich DC, Williams DG. 2004. Hydraulic redistribution
696 by a dominant, warm-desert phreatophyte: seasonal patterns and response to
697 precipitation pulses. *Functional Ecology* **18**:530-538. DOI: 10.1111/j.0269-
698 8463.2004.00867.x.

699 Hultine KR, Williams DG, Burgess SSO, Keefer TO. 2003b. Contrasting patterns of
700 hydraulic redistribution in three desert phreatophytes. *Oecologia* **135**:167-175.

701 Huxman TE, Cable JM, Ignace DD, Eilts JA, English NB, Weltzin J, Williams DG. 2004a.
702 Response of net ecosystem gas exchange to a simulated precipitation pulse in a semi-
703 arid grassland: the role of native versus non-native grasses and soil texture. *Oecologia*
704 **141**:295–305. DOI: 10.1007/s00442-003-1389-y.

705 Huxman TE, Snyder KA, Tissue D, Leffler AJ, Ogle K, Pockman WT, Sandquist DR, Potts
706 DL, Schwinning S. 2004b. Precipitation pulses and carbon fluxes in semiarid and arid
707 ecosystems. *Oecologia* **141**:254–268. DOI: 10.1007/s00442-004-1682-4.

708 Jameson J. 2012. *The importance of biological soil crust in Australian semi-arid ecosystems*.
709 B.Sc. (Honours). University of Technology, Sydney, Sydney, NSW, Australia.

710 Lauenroth WK, Schlaepfer DR, Bradford JB. 2014. Ecohydrology of Dry Regions: Storage
711 versus Pulse Soil Water Dynamics. *Ecosystems* **17**:1469-1479. DOI: 10.1007/s10021-
712 014-9808-y.

713 Lin H. 2010. Earth's Critical Zone and hydropedology: concepts, characteristics, and
714 advances. *Hydrology and Earth System Sciences* **14**:25-45.

715 Lin H. 2011. Three principles of soil change and pedogenesis in time and space. *Soil Science*
716 *Society of America Journal* **75**:2049-2070. DOI: 10.2136/sssaj2011.0130.

717 Litchfield WH, Mabbutt JA. 1962. Hardpan in soils of semi-arid Western Australia. *Journal*
718 *of Soil Science* **13**:148-159.

719 Loik ME, Breshears DD, Lauenroth WK, Belnap J. 2004. A multi-scale perspective of water
720 pulses in dryland ecosystems: climatology and ecohydrology of the western USA.
721 *Oecologia* **141**:269–281.

722 Ludwig F, Dawson TE, de Kroon H, Berendse F, Prins HHT. 2003. Hydraulic lift in *Acacia*
723 *tortilis* trees on an East African savanna. *Oecologia* **134**:293-300. DOI:
724 10.1007/s00442-002-1119-x.

725 Ludwig JA, Wilcox BP, Breshears DD, Tongway DJ, Imeson AC. 2005. Vegetation patches
726 and runoff-erosion as interacting ecohydrological processes in semiarid landscapes.
727 *Ecology* **86**:288–297.

728 Ma X, Huete A, Yu Q, Restrepo Coupe N, Davies K, Broich M, Ratana P, Beringer J, Hutley
729 LB, Cleverly J, Boulain N, Eamus D. 2013. Spatial patterns and temporal dynamics in
730 savanna vegetation phenology across the North Australian Tropical Transect. *Remote*
731 *Sensing of Environment* **139**:97–115. DOI: 10.1016/j.rse.2013.07.030.

732 Maes WH, Minchin PEH, Snelgar WP, Steppe K. 2014. Early detection of Psa infection in
733 kiwifruit by means of infrared thermography at leaf and orchard scale. *Functional*
734 *Plant Biology* **41**:1207-1220. DOI: 10.1071/fp14021.

735 Martin HA. 2006. Cenozoic climatic change and the development of the arid vegetation in
736 Australia. *Journal of Arid Environments* **66**:533–563. DOI:
737 10.1016/j.jaridenv.2006.01.009.

738 Massman W, Clement R. 2004. Uncertainty in eddy covariance flux estimates resulting from
739 spectral attenuation. Pages 67–100 *in* Lee X, Massman W, and Law B, editors.
740 *Handbook of Micrometeorology: A guide for Surface Flux Measurement and Analysis*.
741 Kluwer Academic Publishers, Dordrecht/Boston/London.

742 Migliavacca M, Reichstein M, Richardson AD, Mahecha MD, Cremonese E, Delpierre N,
743 Galvagno M, Law BE, Wohlfahrt G, Black TA, Carvalhais N, Ceccherini G, Chen JQ,
744 Gobron N, Koffi E, Munger JW, Perez-Priego O, Robustelli M, Tomelleri E, Cescatti
745 A. 2015. Influence of physiological phenology on the seasonal pattern of ecosystem

746 respiration in deciduous forests. *Global Change Biology* **21**:363-376. DOI:
747 10.1111/gcb.12671.

748 Mohawesh O, Ishida T, Fukumura K, Yoshino K. 2008. Assessment of spatial variability of
749 penetration resistance and hardpan characteristics in a cassava field. *Australian*
750 *Journal of Soil Research* **46**:210-218. DOI: 10.1071/sr07118.

751 Moreno-de las Heras M, Saco PM, Willgoose GR, Tongway DJ. 2012. Variations in
752 hydrological connectivity of Australian semiarid landscapes indicate abrupt changes in
753 rainfall-use efficiency of vegetation. *Journal of Geophysical Research* **117**:G03009.
754 DOI: 10.1029/2011jg001839.

755 Morton SR, Smith DMS, Dickman CR, Dunkerley DL, Friedel MH, McAllister RRJ, Reid
756 JRW, Roshier DA, Smith MA, Walsh FJ, Wardle GM, Watson IW, Westoby M. 2011.
757 A fresh framework for the ecology of arid Australia. *Journal of Arid Environments*
758 **75**:313–329. DOI: 10.1016/j.jaridenv.2010.11.001.

759 Murphy BP, Paron P, Prior LD, Boggs GS, Franklin DC, Bowman D. 2010. Using
760 generalized autoregressive error models to understand fire-vegetation-soil feedbacks
761 in a mulga-spinifex landscape mosaic. *Journal of Biogeography* **37**:2169-2182. DOI:
762 10.1111/j.1365-2699.2010.02359.x.

763 Neumann RB, Cardon ZG. 2012. The magnitude of hydraulic redistribution by plant roots: a
764 review and synthesis of empirical and modeling studies. *New Phytologist* **194**:337-
765 352. DOI: 10.1111/j.1469-8137.2012.04088.x.

766 Nix HA, Austin MP. 1973. Mulga: a bioclimatic analysis. *Tropical Grasslands* **7**:9–20.

767 Ogle K, Reynolds JF. 2004. Plant responses to precipitation in desert ecosystems: integrating
768 functional types, pulses, thresholds, and delays. *Oecologia* **141**:282–294. DOI:
769 10.1007/s00442-004-1507-5.

770 Page GFM, Merchant A, Grierson PE. 2016. Inter-specific differences in the dynamics of
771 water use and pulse-response of co-dominant canopy species in a dryland woodland.
772 *Journal of Arid Environments* **124**:332-340. DOI: 10.1016/j.jaridenv.2015.09.004.

773 Porporato A, Daly E, Rodriguez-Iturbe I. 2004. Soil water balance and ecosystem response to
774 climate change. *American Naturalist* **164**:625-632. DOI: 10.1086/424970.

775 Poulter B, Frank D, Ciais P, Myneni RB, Andela N, Bi J, Broquet G, Canadell JG, Chevallier
776 F, Liu YY, Running SW, Sitch S, van der Werf GR. 2014. Contribution of semi-arid
777 ecosystems to interannual variability of the global carbon cycle. *Nature* **509**:600–603.
778 DOI: 10.1038/nature13376.

779 Pressland AJ. 1973. Rainfall partitioning by an arid woodland (*Acacia aneura* F. Muell) in
780 south-western Queensland. *Australian Journal of Botany* **21**:235-245. DOI:
781 10.1071/bt9730235.

782 Pressland AJ. 1976a. Effect of stand density on water-use of mulga (*Acacia aneura* F. Muell)
783 woodlands in southwestern Queensland. *Australian Journal of Botany* **24**:177-191.
784 DOI: 10.1071/bt9760177.

785 Pressland AJ. 1976b. Soil moisture redistribution as affected by throughfall and stemflow in
786 an arid zone shrub community. *Australian Journal of Botany* **24**:641-649. DOI:
787 10.1071/bt9760641.

788 Prieto I, Martinez-Tilleria K, Martinez-Manchego L, Montecinos S, Pugnaire FI, Squeo FA.
789 2010. Hydraulic lift through transpiration suppression in shrubs from two arid
790 ecosystems: patterns and control mechanisms. *Oecologia* **163**:855-865. DOI:
791 10.1007/s00442-010-1615-3.

792 Prieto I, Ryel RJ. 2014. Internal hydraulic redistribution prevents the loss of root conductivity
793 during drought. *Tree Physiology* **34**:39-48. DOI: 10.1093/treephys/tpt115.

794 Pugnaire FI, Haase P, Puigdefabregas J. 1996. Facilitation between higher plant species in a
795 semiarid environment. *Ecology* **77**:1420-1426. DOI: 10.2307/2265539.

796 Reynolds JF, Stafford Smith DM, Lambin EF, Turner BL, Mortimore M, Batterbury SPJ,
797 Downing TE, Dowlatabadi H, Fernandez RJ, Herrick JE, Huber-Sannwald E, Jiang H,
798 Leemans R, Lynam T, Maestre FT, Ayarza M, Walker B. 2007. Global desertification:
799 Building a science for dryland development. *Science* **316**:847–851. DOI:
800 10.1126/science.1131634.

801 Ritchie GL, Sullivan DG, Vencill WK, Bednarz CW, Hook JE. 2010. Sensitivities of
802 Normalized Difference Vegetation Index and a green/red ratio index to cotton ground
803 cover fraction. *Crop Science* **50**:1000-1010. DOI: 10.2135/cropsci2009.04.0203.

804 Ryan PR, Delhaize E, Jones DL. 2001. Function and mechanism of organic anion exudation
805 from plant roots. *Annual Review of Plant Physiology and Plant Molecular Biology*
806 **52**:527-560. DOI: 10.1146/annurev.arplant.52.1.527.

807 Schuepp PH. 1993. Tansley review no. 59 Leaf boundary-layers. *New Phytologist* **125**:477-
808 507. DOI: 10.1111/j.1469-8137.1993.tb03898.x.

809 Schwinning S, Sala OE. 2004. Hierarchy of responses to resource pulses in arid and semi-arid
810 ecosystems. *Oecologia* **141**:211–220. DOI: 10.1007/s00442-004-1520-8.

811 Scott RL, Cable WL, Hultine KR. 2008. The ecohydrologic significance of hydraulic
812 redistribution in a semiarid savanna. *Water Resources Research* **44**:W02440.

813 Smucker AJM, McBurney SL, Srivastava AK. 1982. Quantitative separation of roots from
814 compacted soil profiles by the hydropneumatic elutriation system. *Agronomy Journal*
815 **74**:500-503.

816 Stevens RM, Ewenz CM, Grigson G, Conner SM. 2012. Water use by an irrigated almond
817 orchard. *Irrigation Science* **30**:189-200. DOI: 10.1007/s00271-011-0270-8.

818 Thiry M, Milnes AR, Rayot V, Simon-Coincon R. 2006. Interpretation of palaeoweathering
819 features and successive silicifications in the Tertiary regolith of inland Australia.
820 *Journal of the Geological Society* **163**:723–736. DOI: 10.1144/0014-764905-020.

821 Tongway DJ, Ludwig JA. 1990. Vegetation and soil patterning in semiarid mulga lands of
822 Eastern Australia. *Australian Journal of Ecology* **15**:23–34. DOI: 10.1111/j.1442-
823 9993.1990.tb01017.x.

824 Touboul P, Saoudi N, Atallah G, Kirkorian G. 1992. Catheter ablation for atrial-flutter:
825 current concepts and results. *Journal of Cardiovascular Electrophysiology* **3**:641-652.

826 Tsakalotos DE. 1909. The inner friction of the critical zone. *Zeitschrift Fur Physikalische*
827 *Chemie--Stochiometrie Und Verwandtschaftslehre* **68**:32-38.

828 Webb E, Pearman G, Leuning R. 1980. Correction of flux measurements for density effects
829 due to heat and water-vapor transfer. *Quarterly Journal of the Royal Meteorological*
830 *Society* **106**:85–100.

831 Wesely ML. 1970. *Eddy correlation measurements in the atmospheric surface layer over*
832 *agricultural crops*. Ph.D. Dissertation. University of Wisconsin, Madison.

833 Yunusa IAM, Walker RR, Lu P. 2004. Evapotranspiration components from energy balance,
834 sapflow and microlysimetry techniques for an irrigated vineyard in inland Australia.
835 *Agricultural and Forest Meteorology* **127**:93-107. DOI:
836 10.1016/j.agrformet.2004.07.001.

837 Zeppel MJB, Murray BR, Barton C, Eamus D. 2004. Seasonal responses of xylem sap
838 velocity to VPD and solar radiation during drought in a stand of native trees in
839 temperate Australia. *Functional Plant Biology* **31**:461-470. DOI: 10.1071/fp03220.

840

841

842

843

6 Figure legends

Figure 1. Responses of the green:red ratio index (GRRI) to daily total precipitation (grey bars) in the tussock grass understorey (dotted line), Mulga foliage (solid line) and biological crust (dashed line) during (a) spring and early summer 2012 and (b) the following autumn 2013.

Figure 2. Wet season dynamics of net ecosystem photosynthesis (NEP, three-day moving average, solid line) and cumulative precipitation (dashed line) during (a) Summer–Autumn 2013–2014 and (b) Summer–Autumn 2014–2015. Values of NEP larger than zero (horizontal dotted line) represent positive carbon uptake.

Figure 3. Fluctuations of volumetric soil moisture content (θv) at 100 cm depth in hardpan (solid line) and unconsolidated loamy sand (dashed line). Soil porosity was 0.35 ± 0.006 (n = 95, horizontal dotted line). Grey bars represent weekly total precipitation.

Figure 4. Variability in thermal infrared canopy temperature measured from a low-altitude, unmanned aircraft (drone) on 27 March 2014.

Figure 5. Soil moisture profiles measured in replicate arrays beneath bare soil (circles and dashed line) and Mulga (squares and solid line) (a) before (2–11 May 2013) and during (b) a small storm (12–21 May 2013); or (c) during a large storm (15–24 January 2014). Symbols show mean ± standard error. Lines connect measurements within the same sensor array. Values in (b, c) were computed as the average of the delayed peak response, if present. Missing values indicate sensors that were dysfunctional at the time of measurement.

Figure 6. Root density profile measured near the base of Mulga trees (squares and solid line), at the edge of the canopy (open circles and broken line), and in exposed hardpan (bare soil; triangles and dashed line), Symbols show mean ± standard error (N = 294). Symbols at the same depth with the same letter are not significantly different, and symbols marked with an asterisk are significantly different from the root density at 75 cm depth in the same habitat.

Figure 7. Diel pattern of soil moisture content in unconsolidated soil, 100–120 cm depth, during inter-storm (5–8 February 2013, squares and solid line) and intra-storm (5.4 mm; 9–12 February 2013, circles and dashed line) periods. Symbols represent the mean ± standard error for the four days.

873 **Figure 8**. Site schematic of soil moisture measurements (θ, forked symbols), hardpan (HP),
874 unconsolidated soil (US) and the groundwater (regional aquifer). Where depth to to the top of
875 the hardpan was more than one metre, top-of-hardpan depth was indeterminate; otherwise, the
876 top-of-hardpan contour (dashed line) was inferred from θ during wet conditions. The depth to
877 the base of the hardpan was unknown (deeper than two metres, not as deep as the regional
878 aquifer). No measurements were made below the hardpan. Daily soil moisture drawdown
879 shown in Figure 7 occurred at the location marked by an asterisk. Illustration is not drawn to
880 scale to emphasise measurement depths.

881

882 **Tables**

883 **Table 1**. Historical precipitation statistics.

Year	Precipitation (mm yr^{-1})
1900–2012	254*
1900–1969	231*
1970–2012	316*
Five wettest	
1974	955
2010	833
2000	743
1975	676
1904	555
Five driest	
1928	25
1961	70
1964	76
1965	77
1994	97

884 *median

885

886

887 **Table 2**. Midday (10.00–14.00) air temperature measured at two metres height,

888 sensible heat flux and average daily net ecosystem productivity (NEP) (± standard error).

889 Days when precipitation occurred were not included.

Season	Period	Air temperature (°C)	Sensible heat flux (W m^{-2})	NEP (gC m^{-2} d^{-1})
Summer	21 January–10 February 2014	34.1 ± 0.2	307.1 ± 6.7	−1.00 ± 0.12
Autumn	6–23 March 2014	33.2 ± 0.2	302.2 ± 5.6	0.52 ± 0.06
Summer	21 January–10 February 2015	33.5 ± 0.2	270.4 ± 5.4	1.23 ± 0.07
Autumn	6–23 March 2015	34.0 ± 0.3	367.3 ± 5.3	0.23 ± 0.04

890

891

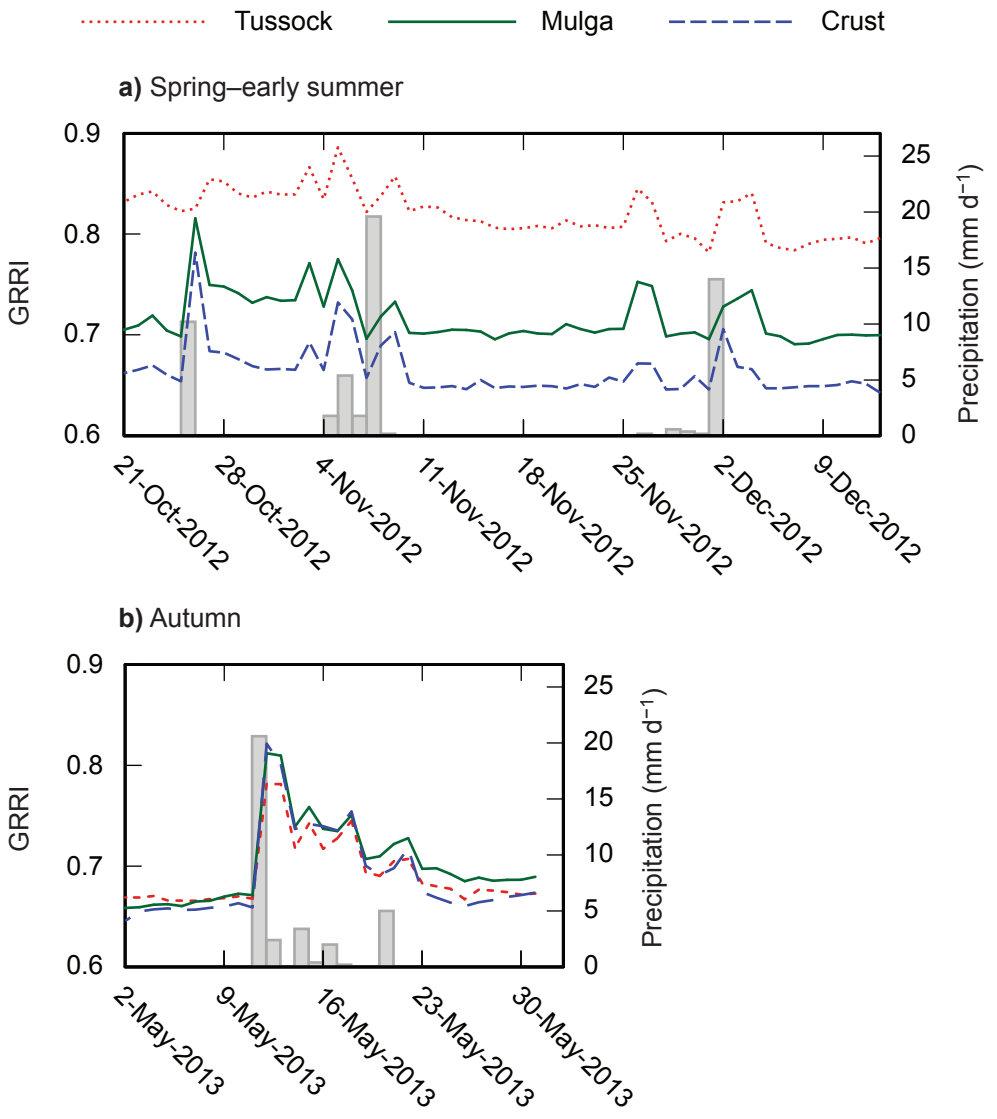

Figure 1. Responses of the green:red ratio index (GRRI) to daily total precipitation (grey bars) in the tussock grass understorey (dotted line), Mulga foliage (solid line) and biological crust (dashed line) during (a) spring and early summer 2012 and (b) the following autumn 2013.

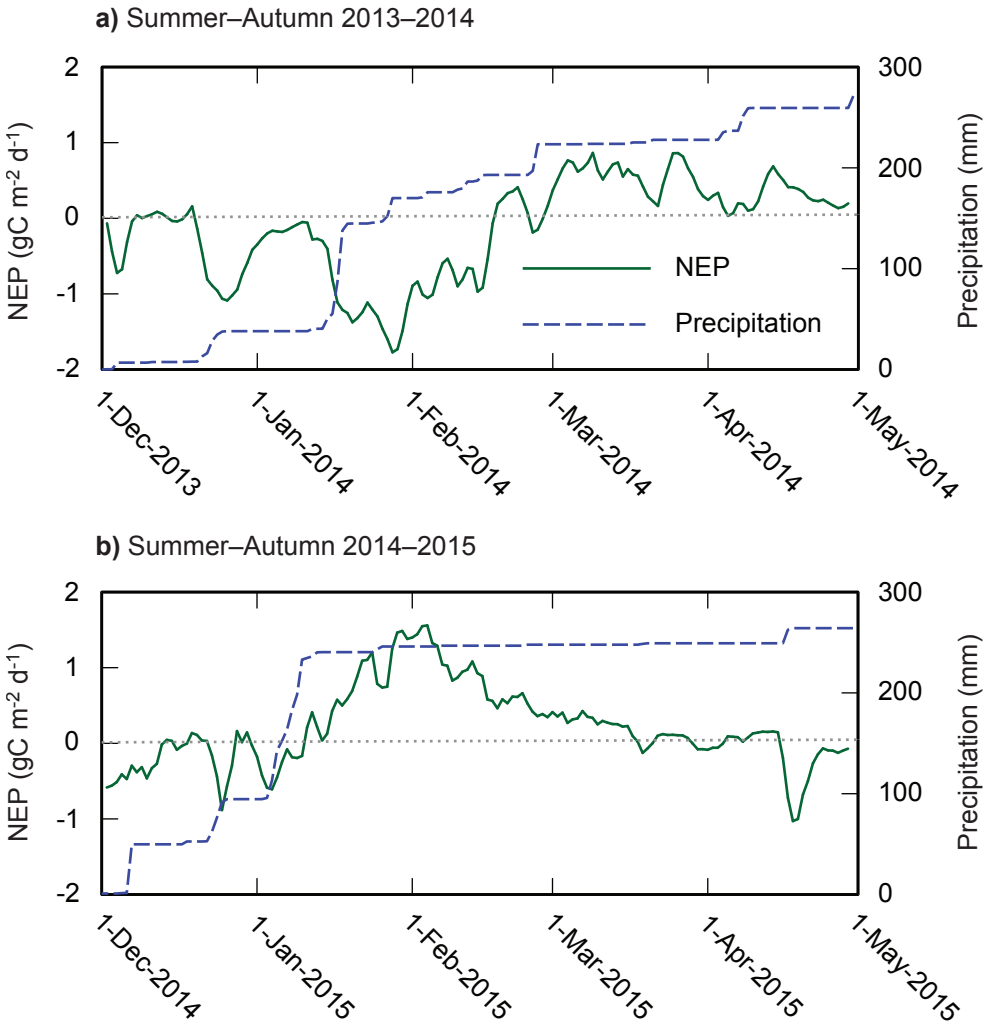

Figure 2. Wet season dynamics of net ecosystem photosynthesis (NEP, three-day moving average, solid line) and cumulative precipitation (dashed line) during (a) Summer–Autumn 2013–2014 and (b) Summer–Autumn 2014–2015. Values of NEP larger than zero (horizontal dotted line) represent positive carbon uptake.

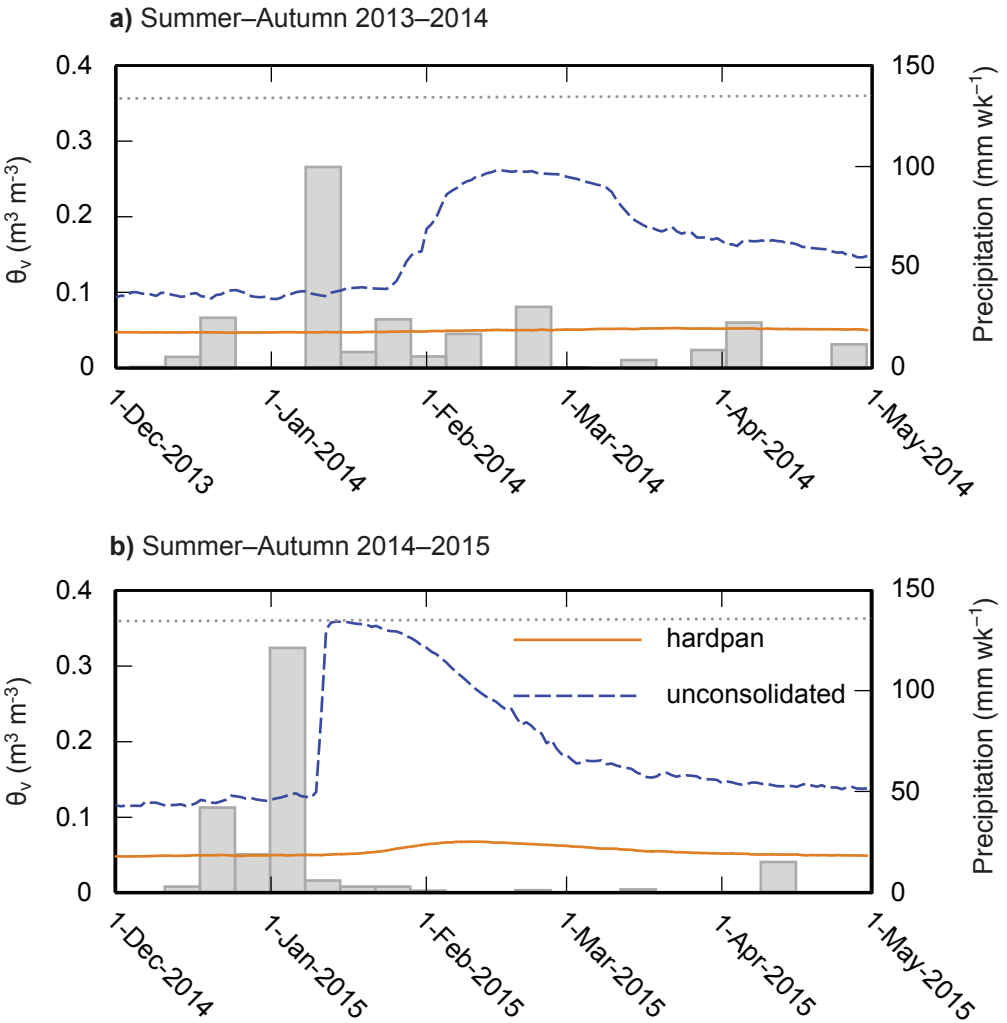

Figure 3. Fluctuations of volumetric soil moisture content (θ_v) at 100 cm depth in hardpan (solid line) and unconsolidated loamy sand (dashed line). Soil porosity was 0.35 ± 0.006 (n = 95, horizontal dotted line). Grey bars represent weekly total precipitation.

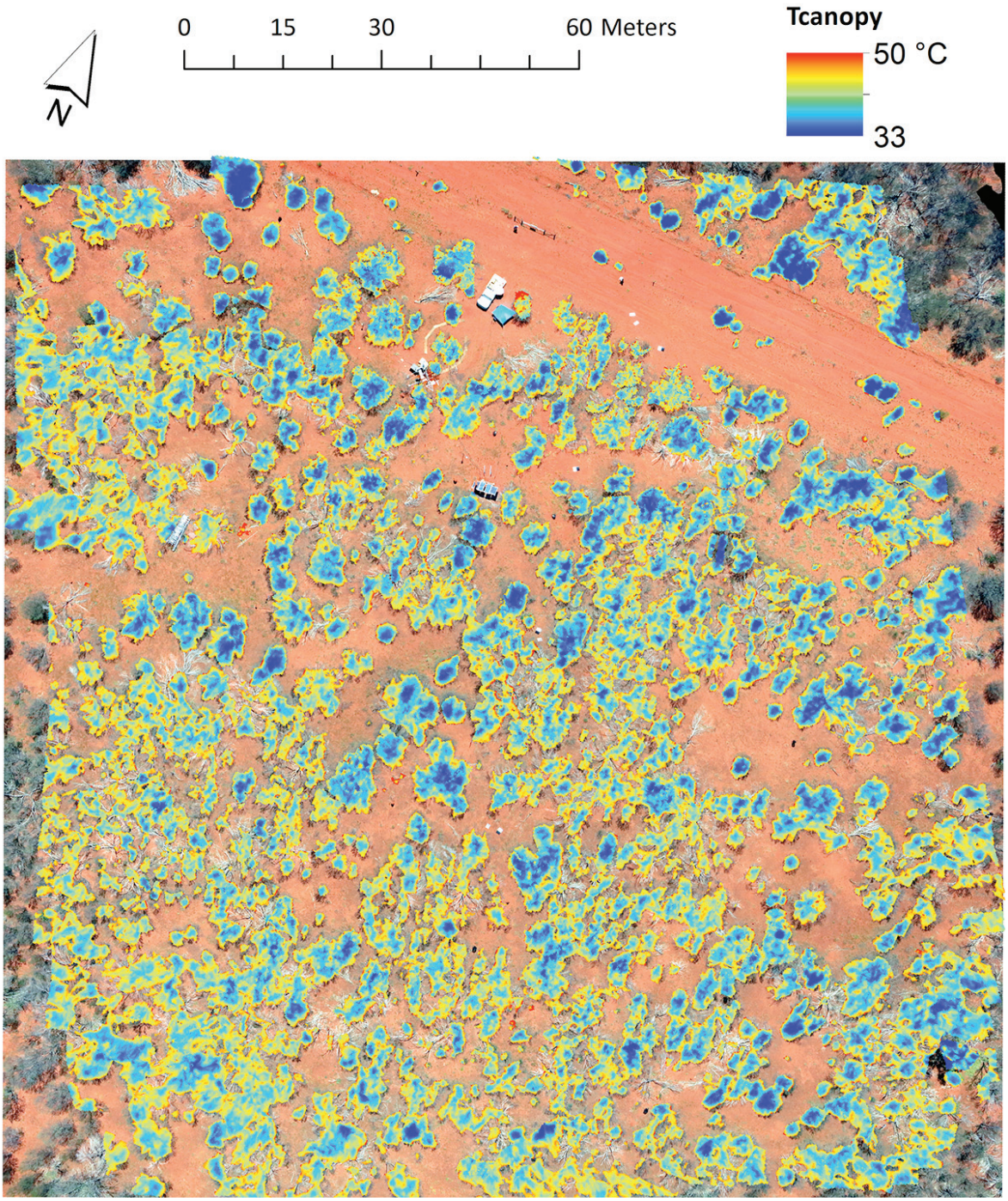

Figure 4. Variability in thermal infrared canopy temperature measured from a low-altitude, unmanned aircraft (drone) on 27 March 2014.

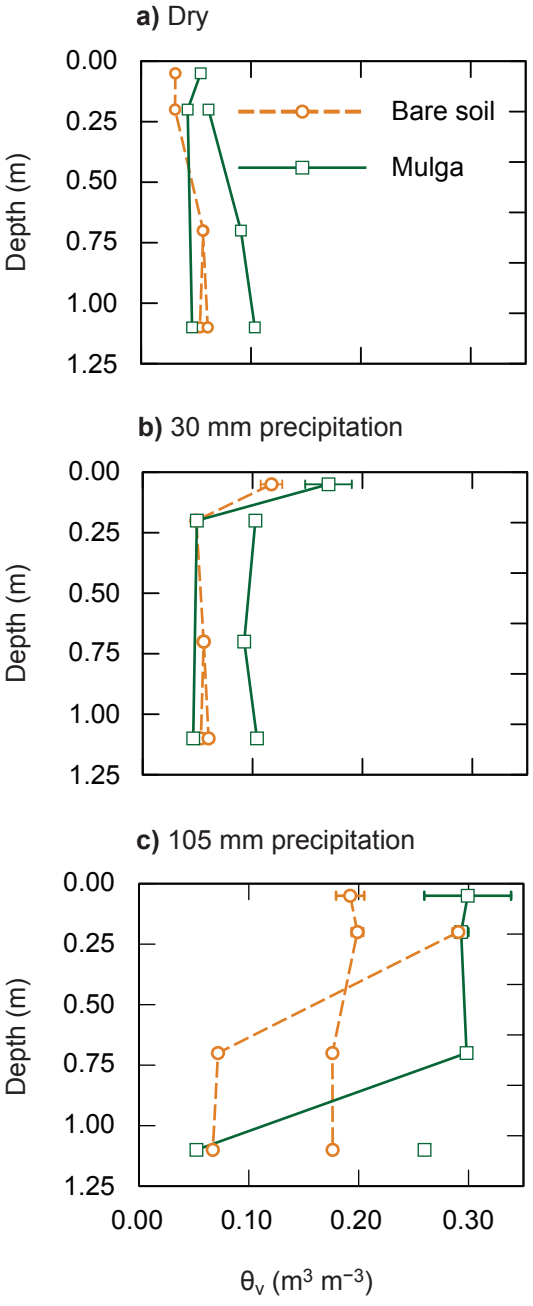

Figure 5. Soil moisture profiles measured in replicate arrays beneath bare soil (circles and dashed line) and Mulga (squares and solid line) (a) before (2–11 May 2013) and during (b) a small storm (12–21 May 2013); or (c) during a large storm (15–24 January 2014). Symbols show mean ± standard error. Lines connect measurements within the same sensor array. Values in (b, c) were computed as the average of the delayed peak response, if present. Missing values indicate sensors that were dysfunctional at the time of measurement.

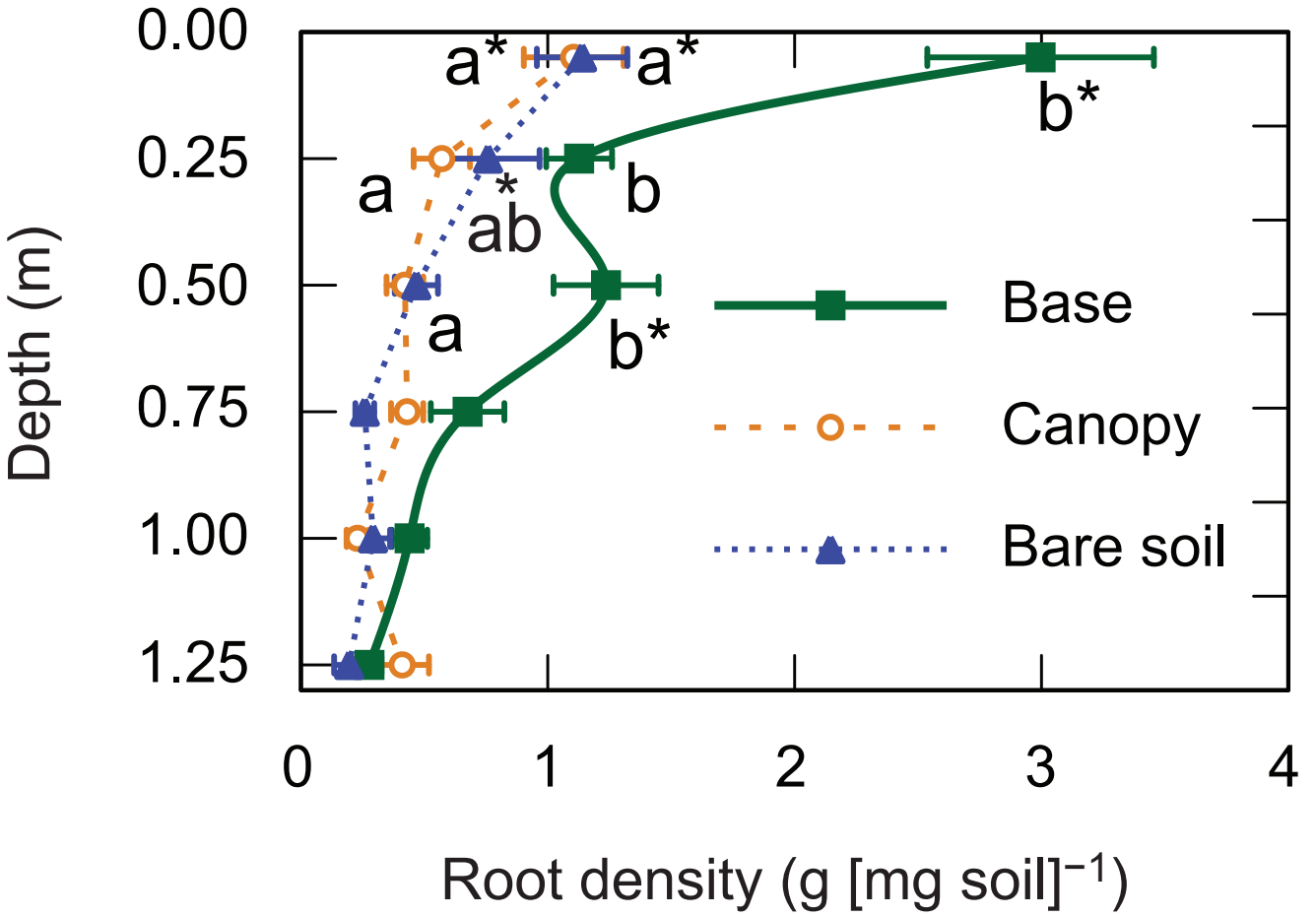

Figure 6. Root density profile measured near the base of Mulga trees (squares and solid line), at the edge of the canopy (open circles and broken line), and in exposed hardpan (bare soil; triangles and dashed line), Symbols show mean ± standard error (N = 294). Symbols at the same depth with the same letter are not significantly different, and symbols marked with an asterisk are significantly different from the root density at 75 cm depth in the same habitat.

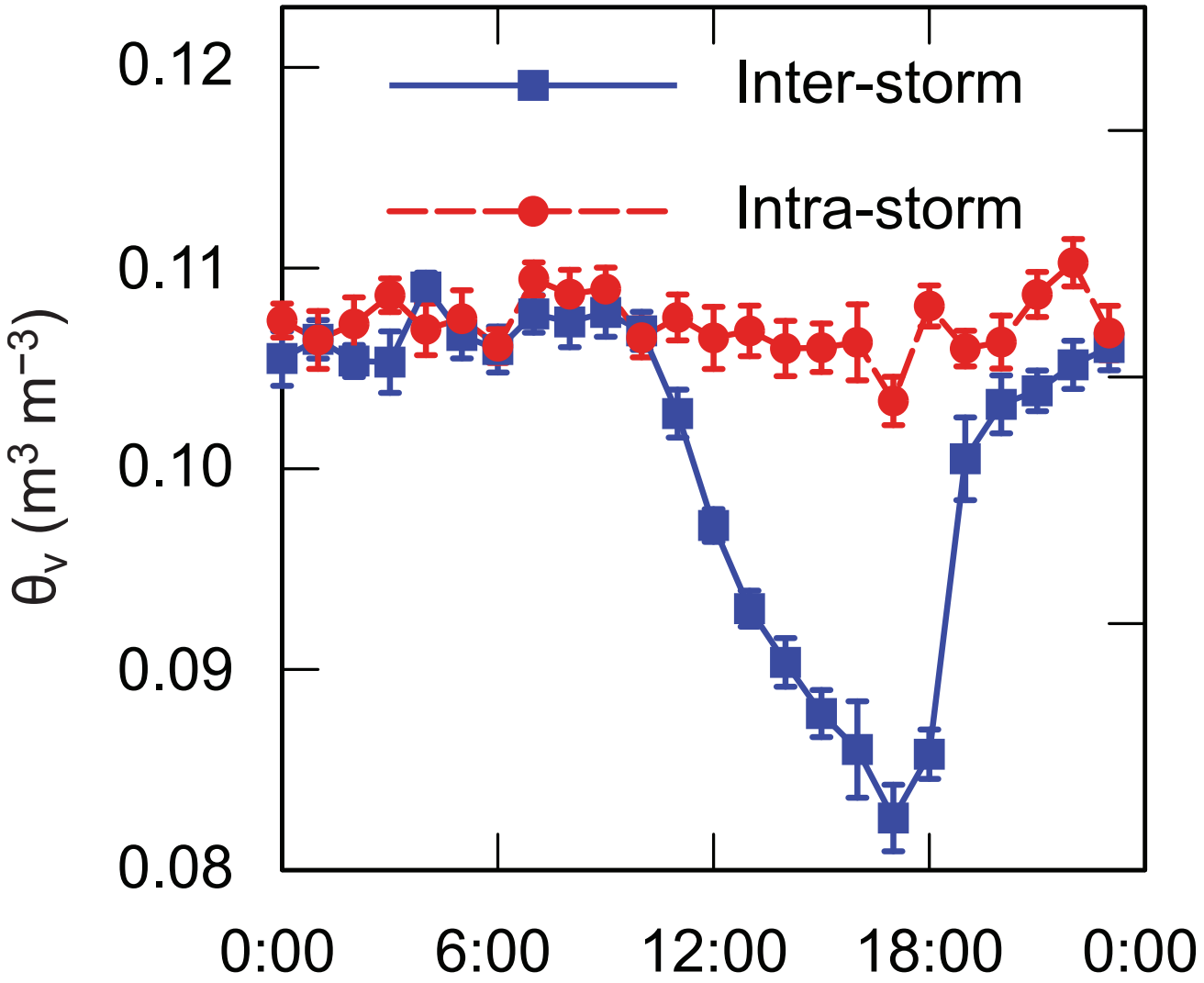

Figure 7. Diel pattern of soil moisture content in unconsolidated soil, 100–120 cm depth, during inter-storm (5–8 February 2013, squares and solid line) and intra-storm (5.4 mm; 9–12 February 2013, circles and dashed line) periods. Symbols represent the mean ± standard error for the four days.

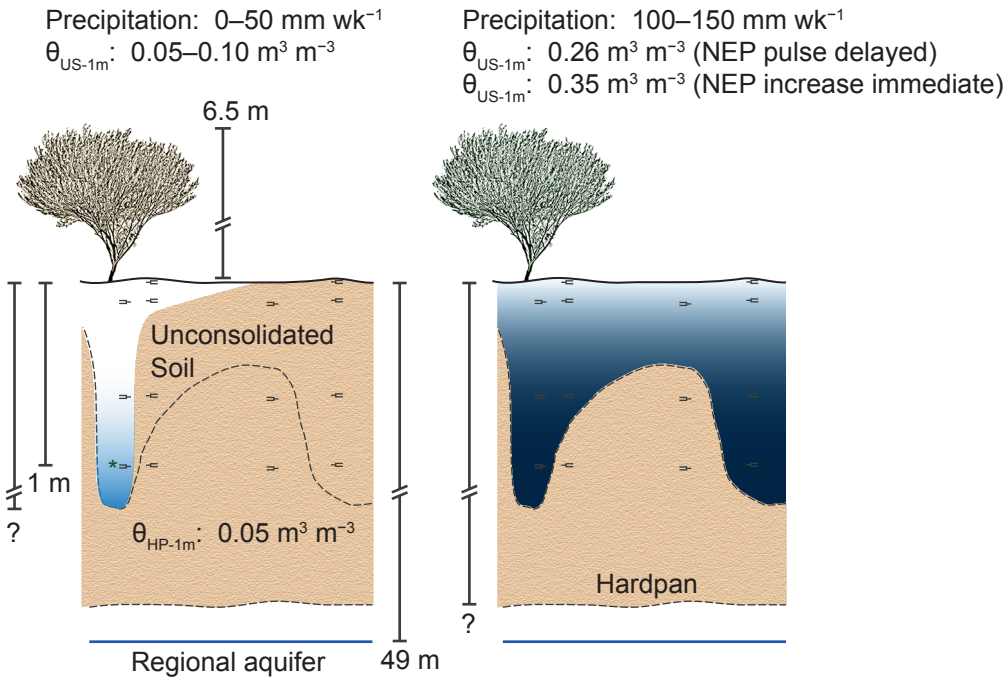

Figure 8. Site schematic of soil moisture measurements (θ, forked symbols), hardpan (HP), unconsolidated soil (US) and the groundwater (regional aquifer). Where depth to to the top of the hardpan was more than one metre, top-of-hardpan depth was indeterminate; otherwise, the top-of-hardpan contour (dashed line) was inferred from θ during wet conditions. The depth to the base of the hardpan was unknown (deeper than two metres, not as deep as the regional aquifer). No measurements were made below the hardpan. Daily soil moisture drawdown shown in Figure 7 occurred at the location marked by an asterisk. Illustration is not drawn to scale to emphasise measurement depths.